Lipopolysaccharide-Induced Expression of Multiple Alternatively Spliced *MEFV* Transcripts in Human Synovial Fibroblasts

A Prominent Splice Isoform Lacks the C-Terminal Domain That Is Highly Mutated in Familial Mediterranean Fever

Arturo Diaz,[1] Chunbo Hu,[1] Daniel L. Kastner,[2] Philip Schaner,[1] Anthony M. Reginato,[3] Neil Richards,[1] and Deborah L. Gumucio[1]

Objective. **To investigate the expression of the familial Mediterranean fever (FMF) gene (*MEFV*) in human synovial fibroblasts.**

Methods. **MEFV messenger RNA in synovial fibroblasts, chondrocytes, and peripheral blood leukocytes (PBLs) was analyzed by semiquantitative and real-time polymerase chain reaction and ribonuclease protection assay. The subcellular localization of pyrin, the *MEFV* product, was determined in transfected synovial fibroblasts and HeLa cells with plasmids encoding pyrin isoforms. Native pyrin was detected with an antipyrin antibody.**

Results. **MEFV was expressed in synovial fibroblasts, but not in chondrocytes. Four alternatively spliced transcripts were identified: an extension of exon 8 (exon 8ext) resulting in a frameshift that predicts a truncated protein lacking exons 9 and 10, the addition of an exon (exon 4a) predicting a truncated protein at exon 5, the in-frame substitution of exon 2a for exon 2, and the previously described removal of exon 2 (exon 2Δ). Exon 8ext transcripts represented 27% of the total message population in synovial fibroblasts. All other alternatively spliced transcripts were rare. Consensus and alternatively spliced transcripts were induced by lipopolysaccharide in synovial fibroblasts and PBLs. In transfected cells, the proteins encoded by all highly expressed splice forms were cytoplasmic. In contrast, native pyrin was predominantly nuclear in synovial fibroblasts, neutrophils, and dendritic cells, but was cytoplasmic in monocytes.**

Conclusion. **Several *MEFV* transcripts are expressed and inducible in synovial fibroblasts. A prominent isoform lacks the C-terminal domain that contains the majority of mutations found in patients with FMF. While recombinant forms of all major pyrin isoforms are cytoplasmic, native pyrin is nuclear in several cell types. Thus, mechanisms in addition to splicing patterns must control pyrin's subcellular distribution.**

Familial Mediterranean fever (FMF) (MIM no. 249100) is the most common of a newly recognized group of diseases characterized by recurrent episodes of inflammation. Because of the lack of an apparent trigger and of a specific immune response, these conditions are defined as autoinflammatory syndromes (1,2). In the recent past, molecular approaches have identified gene mutations that have helped to better define many of these conditions, including FMF, tumor necrosis factor

receptor–associated periodic syndrome (TRAPS) (3), familial cold urticaria (FCU) (4), Muckle-Wells syndrome (MWS) (5), neonatal-onset multisystem inflammatory disease/chronic infantile neurologic, cutaneous, articular syndrome (NOMID/CINCA syndrome), (6), hyperimmunoglobulinemia D with periodic fever syndrome (HIDS) (7,8), pyogenic sterile arthritis, pyoderma gangrenosum and arthritis syndrome (PAPA syndrome) (9), and Blau syndrome (10).

FMF is an autosomal-recessive disease that is prevalent in the Mediterranean basin, affecting people of Jewish, Armenian, Turkish, and Arab ancestry. It is characterized by apparently spontaneous and recurrent episodes of fever and painful serosal inflammation involving the pleura, pericardium, peritoneum, and synovium; other tissues may be affected less frequently. The arthritis of FMF is characterized by episodes of acute monarthritis, although rarely, patients will develop a chronic arthropathy with osteopenia and bone erosions. During the attacks, there is elevation of the leukocyte count, erythrocyte sedimentation rate, and acute-phase reactant levels; the leukocyte count in the synovial fluid can reach values as high as $1,000,000/mm^3$. The most significant late complication of FMF is amyloidosis, which results in chronic renal insufficiency (11,12).

MEFV was cloned in 1997 (13,14). It spans a 15-kb interval on chromosome 16p, contains 10 exons that comprise a 3. 7-kb transcript, and encodes a 781–amino acid protein named pyrin (13) or marenostrin (14), hereinafter referred to as pyrin. Pyrin contains several identifiable domains: a pyrin domain at the N-terminus, a bZIP transcription factor basic domain, a B box–type zinc finger, 2 putative nuclear localization signals, a coiled-coil domain, and a C-terminal domain known as a B30.2, rfp, or SPRY domain. Approximately 40 mutations have been identified in FMF patients, most of them localized in the B30.2/rfp/SPRY domain. Pyrin is the founding member of a growing family of proteins containing a pyrin domain (also known as DAPIN, PAAD, or PYD) (15–17), a death domain–like structure known to interact with other pyrin domain–containing proteins, such as ASC, that are involved in the regulation of apoptosis and NF-κB activation (18). Pyrin has also been shown to interact with PSTPIP1/CD2BP1, the protein mutated in PAPA syndrome, providing a link between the actin cytoskeleton, protein phosphorylation, and the inflammatory process (9,19).

Although the role of pyrin in inflammation has not been elucidated, the fact that mutations are associated with spontaneous inflammatory attacks indicates that the protein is a relevant regulator of the inflammatory process. The mechanisms that trigger FMF attacks and the underlying reasons for the localization of the ensuing inflammation have yet to be established. Human *MEFV* messenger RNA (mRNA) is expressed in polymorphonuclear cells (PMNs), eosinophils, and monocytes, but absent from lymphocytes (13,14,20). It is possible that FMF attacks reflect abnormal trafficking of PMNs or altered chemotactic signaling from monocyte/macrophages. However, structural cells at the site of the targeted inflammation could also be involved in attack localization. Matzner et al (21) showed that pyrin is indeed expressed in skin and peritoneal fibroblasts. Although early studies indicated that *MEFV* mRNA could also be amplified from synovium by reverse transcriptase–polymerase chain reaction (RT-PCR) (14), the regulation of the *MEFV* transcript and pyrin protein in this tissue has not been previously analyzed.

In the present study we investigated the expression of *MEFV* in human synovial fibroblasts treated with the proinflammatory stimulus lipopolysaccharide (LPS) and determined the subcellular localization of the recombinant and native pyrin proteins. Our data demonstrate that pyrin is expressed and inducible in the synovium, an important target site of FMF attacks. We identified transcripts with alternative splicing events at exon 2, exon 4, and exon 8 in synovial fibroblasts and peripheral blood leukocytes (PBLs); only the latter was expressed at significant levels. We found that in transfected synovial fibroblasts, full-length pyrin protein has a cytoplasmic localization, as do all but 1 of the predicted protein isoforms; only the rare isoform encoded by transcripts lacking exon 2 was occasionally nuclear. However, native pyrin had a predominantly nuclear localization in synovial fibroblasts, PMNs, and dendritic cells (DCs), although it was cytoplasmic in monocytes. These findings imply previously unrecognized complexity in the posttranscriptional processing of *MEFV*.

MATERIALS AND METHODS

Cell culture. Primary human synovial fibroblasts (passages 4–10) were obtained from patients with osteoarthritis (OA) as previously described (22) and cultured with Dulbecco's modified Eagle's medium (DMEM) supplemented with heat-inactivated 10% human serum and 10% fetal bovine serum (FBS), L-glutamine, and 1% (volume/volume) penicillin/streptomycin. Unfractionated PBLs were obtained from healthy volunteers (University of Michigan Institutional Review Board nos. 2000-0789 and 2000-0784) who were not taking any drugs. PBLs were separated in Ficoll gradients (Histopaque 1077; Sigma, St. Louis, MO). Unfractionated PBLs were cultured under nonadherent conditions in poly-HEME (Sigma)–covered 100-mm culture dishes, in 10% heat-inactivated FBS. In some experiments, PMNs and monocytes were enriched by Ficoll gradient or cell adhesion. Synovial

fibroblasts and PBLs were incubated for various amounts of time in the presence or absence of various concentrations of LPS (from *Escherichia coli* serotype O127:B8; Sigma). Chondrocytes were obtained from human adult OA cartilage, cultured as previously described (23), and incubated for 24 hours with LPS (30 ng/ml), interleukin-1β (IL-1β; 1 ng/ml), or tumor necrosis factor α (TNFα; 5 ng/ml) (R&D Systems, Minneapolis, MN). Human umbilical vein endothelial cells (HUVECs) were cultured as described (24) and incubated for 24 hours with TNFα (5 ng/ml). HeLa cells (American Type Culture Collection, Rockville, MD) were cultured in DMEM supplemented with 10% heat-inactivated FBS. Monocyte-derived immature DCs were prepared as previously described (25).

RNA isolation and RT-PCR. Cells were lysed in TRIzol reagent (Invitrogen, Carlsbad, CA), and total RNA was isolated and reverse transcribed with Superscript II RNase H$^-$ reverse transcriptase (Invitrogen). The complementary DNA (cDNA) obtained was amplified by PCR using *Taq* DNA polymerase (Invitrogen) with ^{32}P-dCTP labeling. For amplification of the *MEFV* cDNA, a forward primer anchored in exon 5 (5′-GAACAGCAGGAGCATTTCTTTG) and a reverse primer anchored in exon 10 (5′-TGGTACTAC-TTTTCCTTCATC) were used. PCR products were cloned in the pCR 2.1-TOPO vector (Invitrogen) and sequenced. *MEFV* cDNA containing only the consensus splicing of exons 8/9 or the alternative exon 8ext were amplified using a forward primer anchored in exon 5 (5′-GAACAGCAG-GAGCATTTCTTTG) and a reverse primer anchored at the junction of exons 8/9 (5′-AGCTCTGGAACATTGAACATT) or in the extended region of exon 8 (5′-CAAGTCAAC-AGCACAAGGGA). *MEFV* cDNA containing exon 2 or exon 2Δ was amplified using a forward primer anchored in exon 2 (5′-AGAAATTCTCCTGACTCTAG) or a primer anchored at the splice junction of exons 1/3 (5′-AGCCAT-TCAGGGAAGGCCAC) and a reverse primer anchored in exon 5 (5′-ACAAAGAAATGCTCCTGCTGTTC). To assess the equality of template loading, 18S RNA was amplified using a 1:9 mixture of primers:competimers (QuantumRNA Universal 18S Standards; Ambion, Austin, TX). PCR conditions were as follows: 94ºC for 1 minute, 62ºC for 30 seconds, and 72ºC for 30 seconds. PCR products were resolved in 4% nondenaturing polyacrylamide gels and autoradiographed. For semiquantitative PCR, the linear phase of amplification was determined as previously described (26).

Real-time PCR. Reverse-transcribed RNA was digested with RNase H and used as a template for real-time PCR. Reactions were run in an I-Cycler (Sigma) using SYBR Green as a reporter and Platinum *Taq* Polymerase (Invitrogen). PCR mixes contained 50 ng of cDNA (total RNA equivalent); the annealing temperature and the MgCl concentration were optimized for each primer set. Each sample was run in triplicate, and all runs were performed at least twice. Primers were designed using the Beacon Designer 2.05 program (Premier Biosoft International, Palo Alto, CA). For amplification of *MEFV* cDNA containing the consensus exon 8/9 splicing, a 95-bp product was obtained with a forward primer anchored in exon 7 (5′-CTCCTCCACCAGAAG-TCAG) and a reverse primer anchored at the splice junction of exon 8/9 (5′-AGCTCTGGAACATTGAACATT); the conditions were as follows: 95ºC for 2 minutes, and 40 cycles of 95ºC for 30 seconds, 53ºC for 30 seconds, and 72ºC for 10 seconds.

For amplification of *MEFV* cDNA containing the exon 8ext, a 158-bp product was obtained with a forward primer anchored in exon 7 (5′-CAAGTCAACAGCACAAGGGAACAC) and a reverse primer anchored in the extended region of exon 8 (5′-AGCTCTGGAACATTGAACATT); the conditions were as follows: 95ºC for 2 minutes, and 40 cycles of 95ºC for 30 seconds, 58.4ºC for 30 seconds, and 72ºC for 10 seconds. To normalize for template loading, reverse-transcribed 18S RNA was amplified using a 1:9 primer:competimer mix; the conditions were as follows: 95ºC for 2 minutes, and 40 cycles of 95ºC for 30 seconds, 59.8ºC for 30 seconds, and 72ºC for 10 seconds.

Standard curves were generated using triplicates of progressive 10-fold dilutions of plasmids containing the target *MEFV* or 18S sequences, starting at 10^{-12} mM DNA. The dynamic range of the standard curves spanned 4 orders of magnitude, with correlation coefficients of at least 0.95 and efficiencies of at least 90%. Molar quantities of starting RNA (cDNA equivalent) were calculated for *MEFV* splice variants and for the corresponding 18S RNA for each sample. The concentration of *MEFV* products was corrected by that of 18S RNA, and the resulting values were expressed as arbitrary units.

Plasmid construction. A cDNA spanning *MEFV* exon 1 to exon 8ext was obtained by RT-PCR using a forward primer anchored in exon 1 (5′-ATGGCTAA-GACCCCTAGTGAC) and a reverse primer anchored in the exon 8ext (5′-CTAAATAGGGCCCCTCAAGT) containing 5′ *Eco* RI and 3′ *Xho* I linkers. We obtained clones containing exon 2a or exon 2Δ. Constructs containing the desired splicing combinations were derived from these 2 clones, a cDNA containing exon 4a and the plasmid V75-1 containing a full-length *MEFV* cDNA. Complementary DNA were excised from the plasmids with *Eco* RI and *Xho* I, cut at a *Kpn* I site in exon 3, gel purified, and selected sequences ligated. All cDNA were cloned in the plasmid pCMV–Tag 3A (Stratagene, La Jolla, CA). A plasmid containing 18S sequences was prepared by cloning the RT-PCR product obtained with the primer:competimer mix, in the pCR 2.1-TOPO vector.

RNase protection assays. For analysis of exon 2 splicing, a riboprobe was generated from a 5′ linearized plasmid containing 493 bp of *MEFV* coding sequences, from the ATG (position 1) in exon 1 to the 472 position in exon 2 and cloned in pCR2.1-TOPO plasmid. After hybridization and RNase digestion, exon 2–containing transcripts resolve as a 493-bp band and exon 2Δ transcripts as a 172-bp band. For analysis of exon 8 splicing, a riboprobe was generated from a plasmid containing *MEFV* coding sequences from the ATG (position 1) to the stop codon in exon 8ext at position 1209. The plasmid was linearized with *Pst* I at the junction of exons 5/6; this generated a 255-bp probe. After hybridization and RNase digestion, the product containing exon 8ext resolves as a 255-bp band and the product with the conventional exon 8/9 splicing runs as a 172-bp band. Riboprobes (α-^{32}P-UTP–labeled) were prepared using the MaxiScript in vitro transcription kit (Ambion). For RNase protection assays (RPAs), 30 μg of total RNA from synovial fibroblasts or 10 μg of total RNA from PBLs was used; RPAs were run at least twice, using the RPA III kit (Ambion). Protected products were resolved by polyacrylamide gel electrophoresis and autoradiographed.

Cellular transfection and protein localization. Synovial fibroblasts were plated on type I collagen–covered glass coverslips (Biocoat; Becton Dickinson, Bedford, MA), and

HeLa cells on standard glass coverslips in 6-well plates. Plated synovial fibroblasts were transfected with 3 μg of DNA using FuGENE reagent (Roche, Indianapolis, IN) or by the nucleofection method using the Human Dermal Fibroblast Nucleofector Kit (Amaxa Biosystems, Cologne, Germany), and then plated. Twenty-four or 48 hours after transfection, cells were fixed for 30 minutes in 4% paraformaldehyde in phosphate buffered saline (PBS), permeabilized for 5 minutes with 0.5% Triton X-100 in PBS, and blocked for 1 hour with 1% bovine serum albumin, 10% goat serum in PBS–0.1% Tween. Primary antibody was mouse monoclonal IgG anti-myc (9E10; Santa Cruz Biotechnology, Santa Cruz, CA). Secondary antibody was goat anti-mouse Alexa Fluor 568–conjugated polyclonal IgG (Molecular Probes, Eugene OR). Cells were incubated for 1 hour with the primary and secondary antibodies diluted in blocking solution. Nuclei were counterstained with 4′,6-diamidino-2-phenylindole (DAPI). Cells were visualized using a Zeiss Axiophot 2 microscope or a Nikon Eclipse E800 microscope. For staining of native pyrin, the primary antibody was a polyclonal rabbit antibody to human pyrin amino acids 1–374 (Ab93). The secondary antibody was a goat anti-rabbit Alexa Fluor 568–conjugated polyclonal IgG (Molecular Probes). Nuclei were counterstained with DAPI or Hoechst. Cells were visualized as described above and with a Zeiss LMS 510 confocal microscope.

RESULTS

Expression of *MEFV* in synovial fibroblasts and identification of an alternatively spliced transcript containing an extension of exon 8. To survey *MEFV* expression in a variety of cell types found in the joint, we used RT-PCR. *MEFV* message was not detected in chondrocytes incubated in medium alone or supplemented for 24 hours with LPS, TNFα, or IL-1β. Likewise, HUVECs (untreated or incubated with TNFα) did not express *MEFV* transcripts. *MEFV* message was detected in DCs and in synovial fibroblasts (Figure 1A); expression in synovial fibroblasts was investigated further.

Semiquantitative RT-PCR of total RNA from synovial fibroblasts, using primers anchored in exons 5 and 10, revealed a 680-bp amplicon, mildly inducible by LPS. Sequencing confirmed that this band contained the expected consensus spliced *MEFV* product. LPS stimulation also caused a dose- and time-dependent stronger induction of a transcript producing a larger (796-bp) amplicon (Figure 1A). Induced transcripts were detected as early as 2 hours. Sequencing of the larger PCR product revealed that it contained an extension of exon 8 (exon 8ext), provided by the first 118 bp of intron 8. This caused a frameshift resulting in multiple stop codons, the first contained within the extension of exon 8, predicting a 613–amino acid truncated protein product lacking exons 9 and 10 and thus missing the entire rfp/SPRY/B30.2 domain (Figures 1B and C).

Semiquantitative RT-PCR using primers that specifically detect only one splice form at a time con-
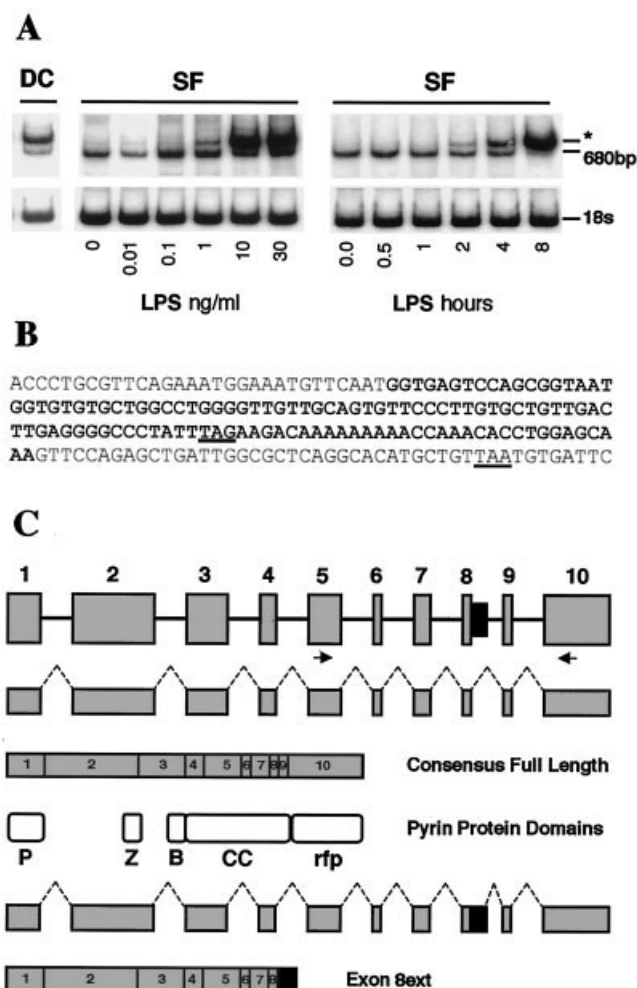
Figure 1. Expression of *MEFV* message in dendritic cells (DCs) and synovial fibroblasts (SFs), and lipopolysaccharide (LPS) induction of an alternatively spliced *MEFV* transcript containing an extension of exon 8 in synovial fibroblasts. **A,** *MEFV* mRNA was analyzed by reverse transcriptase–polymerase chain reaction (PCR) using primers anchored in exons 5 and 10 (arrows in **C**); 18S RNA was amplified as control. PCR products were labeled with ³²P-dCTP and PCR was run for 27 cycles, a point previously determined to be within the linear range of amplification (data not shown). The expected 680-bp *MEFV* product is shown. **Asterisk** indicates a larger induced product. Immature monocyte–derived DCs were studied (left panel). Cultured synovial fibroblasts were incubated with various concentrations of LPS for 24 hours (center panel), or with 30 ng/ml LPS for various amounts of time (right panel). **B,** Partial sequence of the larger PCR product indicated by the asterisk in **A.** Characters in boldface represent the first 118 bp from intron 8 (exon 8ext); this region is flanked by sequences from exons 8 and 9. Underlined are the generated 3′ stop codons within the extended region of exon 8 and exon 9. **C,** Diagram of the *MEFV* gene (top); the introns are not drawn to scale. Exons appear as numbered gray boxes, introns are represented by a black line, and the extension of exon 8 (exon 8ext) is shown as a black box adjacent to exon 8. Below are diagrams of the consensus (middle) and alternatively (bottom) spliced mRNA and their predicted protein products, with the coding exons numbered. Several specific domains found in the pyrin protein are aligned with their coding exons (P = pyrin domain; Z = bZIP domain; B = B box domain; CC = coiled-coil domain; rfp = rfp/B30.2/SPRY domain).

firmed that LPS treatment induced both the consensus and the alternatively spliced transcripts (Figure 2A) and indicated that both transcripts were more abundant in PBLs than in synovial fibroblasts. To demonstrate the existence and estimate the relative abundance of transcripts expressing exon 8ext by an independent technique not dependent on PCR, we performed RPA (Figure 2B); transcripts containing exon 8ext were expressed at low levels in untreated PBLs and undetectable in untreated synovial fibroblasts. Treatment with LPS induced exon 8ext–containing transcripts in both cell populations, but these were less abundant than consensus spliced transcripts.

Quantification of exon 8 splicing products by real-time PCR. To quantify the effect of LPS on the abundance of consensus and exon 8ext–containing transcripts, we performed real-time PCR on synovial fibroblasts from 3 OA patients and PBLs from 3 healthy subjects (Figure 2C). Untreated synovial fibroblasts expressed higher levels (2.6-fold) of consensus transcripts than of alternatively spliced transcripts; treatment with LPS resulted in a coordinated induction of both transcripts (increased 3.8–fold). Exon 8ext transcripts represented 27% of the total (consensus plus alternatively spliced) *MEFV* transcripts in both untreated and LPS-treated synovial fibroblasts.

Untreated PBLs from the 3 unrelated healthy donors contained widely different levels of *MEFV* transcripts. Such individual variability was also documented previously (20). As shown in Figure 2C, in all cases we detected higher levels of consensus transcripts (average 15.7-fold) than of alternatively spliced transcripts. PBLs incubated for 8 hours in medium alone displayed a reduction in the expression of both transcripts (15.5-fold for consensus and 9.5-fold for exon 8ext). This reduction may reflect changes in the cellular environment under tissue culture conditions and/or death of PMNs, known *MEFV*-expressing cells. Treatment of PBLs with LPS for 8 hours resulted in increased induction of both transcripts (4.1-fold for consensus, 4.7-fold for exon 8ext). Although the transcript levels in total PBLs are somewhat "diluted" by the presence of lymphocytes, which do not express pyrin, untreated PBLs incubated for 8 hours expressed higher levels of both transcripts compared with untreated synovial fibroblasts (22-fold for consensus, 6-fold for exon 8ext). The exon 8ext–containing transcripts represented a larger proportion of the total message population in synovial fibroblasts (27%), however, than in PBLs (10%) (Figure 2C).

Splicing of exon 2. Papin et al previously identified an alternatively spliced transcript lacking exon 2 in human PBLs (27). To test whether this exon 2Δ splice form also occurs in synovial fibroblasts, total RNA from
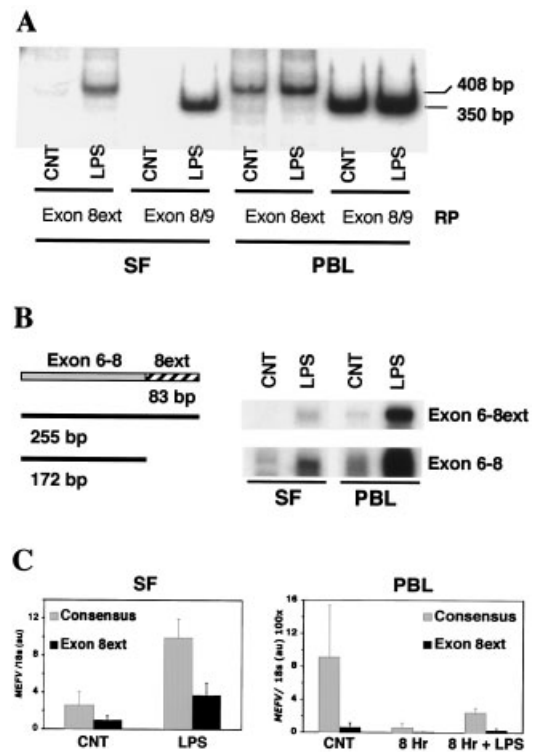
Figure 2. LPS induction of consensus and exon 8ext–containing transcripts in synovial fibroblasts and peripheral blood leukocytes (PBLs). **A,** Cultured synovial fibroblasts (left) or freshly isolated unfractionated PBLs (right) were incubated for 24 hours and 8 hours, respectively, without (control [CNT]) or with LPS (30 ng/ml). Total RNA was assayed for individual *MEFV* splice forms using a common forward PCR primer anchored in exon 5. The reverse primer (RP) to detect consensus spliced *MEFV* (Exon 8/9) spanned the splice junction of exons 8 and 9 and produced a 350-bp product. The reverse primer detecting exon 8ext–containing transcripts was located in the extended region of exon 8 and produced a 408-bp product. PCR amplification was carried out for 27 cycles in the presence of ^{32}P-dCTP. **B,** RNase protection assays. Left, An RNA probe containing sequences from exon 6 to exon 8ext was used to generate protected RNA sequences of 172 bp from consensus spliced pyrin (Exon 6–8) and 255 bp from exon 8ext–containing transcripts (Exon 6–8ext). Right, Autoradiographs of the products resolved by polyacrylamide gel electrophoresis. **C,** Real-time PCR analysis of consensus and exon 8ext–containing transcripts in synovial fibroblasts and PBLs. Synovial fibroblasts from 3 osteoarthritis patients were incubated without (control) or with LPS (30 ng/ml) for 24 hours and total RNA was obtained. Unfractionated PBLs were prepared from 3 healthy donors, and total RNA was obtained at time 0 or after 8 hours of incubation without or with LPS (30 ng/ml). Real-time PCR analysis was performed as described in Materials and Methods. Values are arbitrary units (AU) after normalization of *MEFV* mRNA molar concentrations with 18S RNA molar concentrations as described in Materials and Methods (mean and SD from the 3 synovial fibroblast donors and the 3 PBL donors) (values from individual samples available at http://www.med.umich.edu/cdb/sub_pages/People/gumucio.htm). See Figure 1 for other definitions.

synovial fibroblasts from 3 different individuals, and a monocyte-enriched fraction of PBLs, were analyzed by RT-PCR. LPS treatment of both cell types resulted in
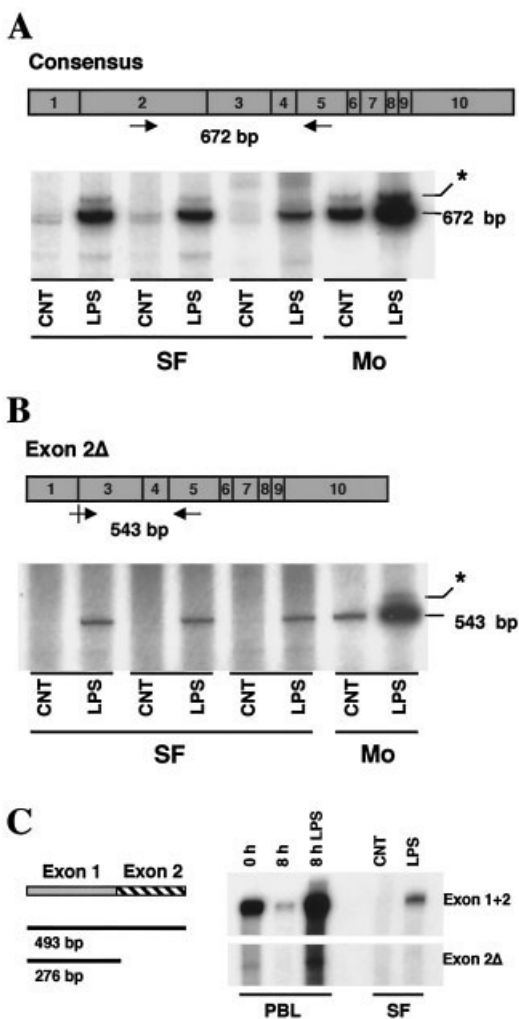
Figure 3. Splicing of exon 2 in synovial fibroblasts and peripheral blood leukocytes (PBLs). **A,** Cultured synovial fibroblasts from 3 subjects were incubated for 24 hours without (control [CNT]) or with LPS (30 ng/ml). Monocyte (Mo)–enriched PBLs from a healthy donor were incubated for 8 hours without or with LPS (30 ng/ml). Total RNA was used for reverse transcriptase–PCR reactions, run for 35 cycles in the presence of ^{32}P-dCTP. The primers used for amplification of consensus spliced *MEFV* were anchored in exon 2 and exon 5 (top); the expected 672-bp product is indicated, along with an additional larger product (**asterisk**). **B,** The primers used for amplification of exon 2Δ transcripts were anchored at the junction of exons 1/3 and in exon 5; the expected 543-bp product is indicated in the autoradiograph, along with an additional larger product (**asterisk**). **C,** Ribonuclease protection assays. Left, A 493-bp probe containing sequences from exons 1 and 2 was used to generate a protected fragment of 493 bp from consensus spliced *MEFV* (Exon 1+2), and a fragment of 276 bp from exon 2Δ transcripts. Right, Autoradiographs of the resolved products. See Figure 1 for other definitions.

synovial fibroblasts, the exon 2Δ message was seen only after LPS stimulation (Figure 3C). The rarity of the Δ2 message and the response to LPS was also demonstrated by RPA (Figure 3C). Analysis by real-time PCR con-

Figure 4. Identification of alternatively spliced *MEFV* transcripts containing exons 4a and 2a. **A,** Exon 4a. The sequence of exon 4a is shown in boldface, flanked by exons 4 and 5. Underlined is the first of a series of generated 3′ stop codons. A diagrammatic representation of the *MEFV* gene is also shown, with exon 4a represented as a black box nested inside intron 4. The generation of the exon 4a protein product and a second product that contains exon 4a but lacks exon 2 (exon 2Δ/4a) is also diagrammed. **B,** Exon 2a. The sequence of exon 2a is shown in boldface, flanked by exons 1 and 3. A diagrammatic representation of the *MEFV* gene is also shown, with exon 2a represented as a black box nested in intron 2. Diagrams of detected alternative splicing events and their resulting protein products, including those containing exon 8ext and exon2a (Exon 2a/8ext) and transcripts containing exon 8ext but not exon 2 (Exon 2Δ/8ext), are also shown.
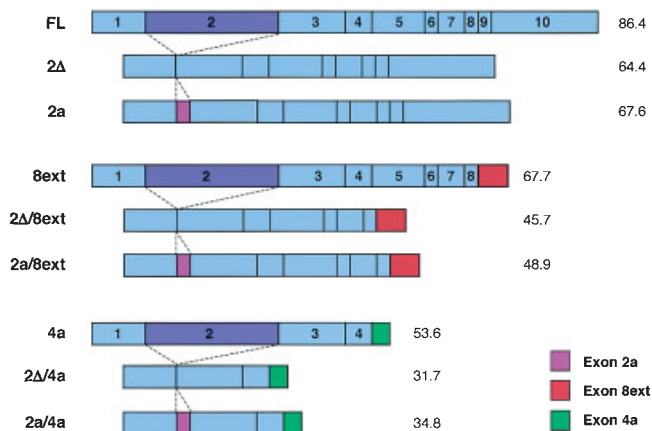
the induction of transcripts containing exon 2 (Figure 3A). Primers spanning the exon 1/3 junction were used to detect transcripts lacking exon 2. This message was detectable in monocytes and inducible with LPS. In

Figure 5. Summary of the alternative splice forms of *MEFV* transcripts in synovial fibroblasts and peripheral blood leukocytes. Horizontal bars represent spliced transcripts, named on the left. The coding exons are numbered. The predicted molecular weights of the predicted translated products (kilodaltons) are on the right. FL = full-length.

firmed that exon 2Δ transcripts were at least 2 orders of magnitude less abundant than transcripts containing exon 2 (results not shown).

We also investigated whether transcripts containing combined splicing events at exon 2 and exon 8 were expressed in synovial fibroblasts and PBLs. Specific primers were designed to detect each isoform individually. Although both cell types produced all 4 possible transcripts (consensus, exon 8ext, 2Δ, and 2Δ/8ext), the latter form was exceedingly rare. A figure depicting these results is available online at http://www.med.umich.edu/cdb/sub_pages/People/gumucio.htm.

Identification of exon 4a. During analysis of exon 2 isoforms, we detected a larger product (asterisk in Figures 3A and B). Sequencing showed that this product contained an extra 98 bp following exon 4, corresponding to a small exon nested in intron 4; hence, it was named
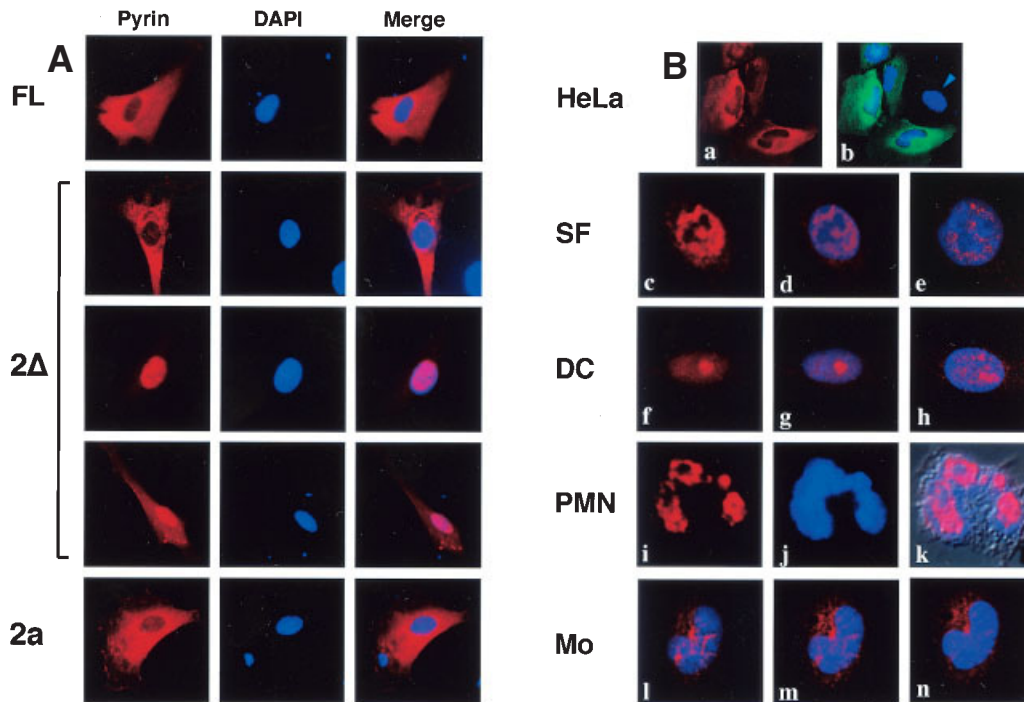
Figure 6. Subcellular localization of recombinant pyrin isoforms and native pyrin. **A,** Synovial fibroblasts were transiently transfected with plasmids encoding myc-tagged full-length pyrin (FL) or pyrin isoforms lacking exon 2 (2Δ) or containing exon 2a, and processed as described in Materials and Methods. Pyrin protein was detected in transfected cells with an anti-myc antibody and visualized in the rhodamine channel (red; left column), nuclei were counterstained with 4′,6-diamidino-2-phenylindole (DAPI) (blue; middle column), and the images were merged (right column). The 3 patterns of subcellular localization detected for exon 2Δ protein are shown in the center 3 bracketed rows as cytoplasmic (top), predominantly nuclear (middle), and mixed cytosolic/nuclear (bottom). **B,** Native pyrin was detected with a polyclonal antipyrin primary antibody and an Alexa Fluor 568 rhodamine–conjugated secondary antibody (red). Nuclei were counterstained with DAPI or Hoechst stain (blue). **a** and **b,** Specificity of the antibody is verified in HeLa cells transfected with myc-pyrin and visualized with **a,** the antipyrin antibody (red) or **b,** an anti-myc monoclonal antibody (green). A nontransfected cell is indicated by the **arrowhead**. **c–e,** Native pyrin in synovial fibroblasts: **c,** pyrin, **d,** merged image of pyrin and DAPI stain, **e,** dual-channel image of the nuclei obtained by confocal microscopy. **f–h,** Native pyrin in DCs: **f,** pyrin, **g,** merged image of pyrin and Hoechst stain, **h,** dual-channel confocal image of the nuclei. **i–j,** Native pyrin in polymorphonuclear cells (PMN): **I,** pyrin, **j,** Hoechst stain, **k,** merged image of pyrin, Hoechst, and differential interference contrast. **l–m,** Sequential confocal slices through a monocyte (Mo), moving from **l,** the top of the cell to **n,** the bottom, showing cytoplasmic reticular staining of pyrin (red). See Figure 1 for other definitions.

exon 4a. Exon 4a is in-frame with exon 4. However, its insertion causes a frameshift at the beginning of exon 5 that results in multiple stop codons (Figure 4A). The predicted product is a 490–amino acid truncated protein lacking exons 5–10, thus missing much of the coiled-coil and the entire rfp/SPRY/B30.2 domain (see Figure 1C). Transcripts containing exon 4a are in low abundance in PBLs and are barely detectable in synovial fibroblasts.

Identification of exon 2a. While sequencing RT-PCR products with combined splicing events, we detected clones containing a small sequence substituting for exon 2. Analysis revealed this to be a 93-bp sequence embedded in intron 2, referred to here as exon 2a. Exon 2a is in-frame, and therefore is likely to result in a full-length translated protein (Figure 4B) with an alternative exon 2. These transcripts are extremely rare (data not shown).

Summary of alternatively spliced *MEFV* transcripts. Overall, in the present study we identified 3 new splice isoforms of *MEFV* mRNA in synovial fibroblasts and PBLs (exon 2a, exon 4a, and exon 8ext) and confirmed the presence of the previously identified exon 2Δ. We have also demonstrated the existence of transcripts containing combined splicing events, resulting in a total of 9 different *MEFV* transcripts (Figure 5).

Subcellular localization of recombinant pyrin isoforms. To determine the subcellular localization of the protein products encoded by the various alternatively spliced *MEFV* transcripts, we performed transient transfections of synovial fibroblasts and HeLa cells, with expression plasmids encoding the myc-tagged pyrin isoforms represented in Figure 5. All protein products encoded by sequences containing exon 2 or exon 2a had a cytoplasmic localization, regardless of whether they contained, at the 3′ end, a consensus splicing (Figure 6A), an exon 8ext, or an exon 4a (figure available at http://www.med.umich.edu/cdb/sub_pages/People/gumucio.htm). Protein products encoded by exon 2Δ forms had cytoplasmic, nuclear, or mixed (nuclear and cytoplasmic) localization, regardless of whether they contained, at the 3′ end, a consensus splicing (Figure 6A), an exon 8ext, or an exon 4a (figure available at http://www.med.umich.edu/cdb/sub_pages/People/gumucio.htm). The same findings were observed in HeLa cells (results not shown).

We determined the frequency of each localization pattern for each pyrin isoform by counting 50–100 transfected cells. This analysis showed that cells transfected with plasmids encoding exon 2Δ proteins more frequently exhibited a mixed localization (average 67%), followed by cytoplasmic localization (average 25%), and

less frequently, an exclusively nuclear localization (average 8%). All other isoforms were 100% cytoplasmic (table available at http://www.med.umich.edu/cdb/sub_pages/People/gumucio.htm).

Subcellular localization of native pyrin. The transcript analysis and transfection experiments indicated that the majority of pyrin protein should be cytoplasmic in synovial fibroblasts as well as PBLs. To test this, we examined a variety of relevant human cell types using an antibody to detect native human pyrin. To confirm the specificity of the antibody, HeLa cells were transfected with myc-pyrin and stained with antipyrin antibody or anti-myc antibody; only transfected cells showed cytoplasmic staining with both antibodies (Figures 6Ba and Bb). Unexpectedly, untreated and LPS-treated synovial fibroblasts stained with antipyrin displayed a predominantly nuclear localization (apparently excluding the nucleolus), with some cytoplasmic staining (Figures 6Bc–e). In widefield surveys, all cells showed identical staining (results not shown). In immature monocyte–derived DC, pyrin presented predominantly as intranuclear clusters (Figures 6Bf–h). PMNs also showed predominantly nuclear staining (Figures 6Bi–k); only in monocytes was pyrin predominantly cytosolic (Figures 6Bl–n), and distributed in a reticular pattern.

DISCUSSION

Most inflammatory episodes in FMF are characterized by massive influx of PMNs to peritoneal, pleural, or synovial membranes. The reason for the targeting of PMNs to these particular sites is not known, but it is possible that local expression of pyrin protein could be involved. Thus, it was important to define whether resident cells in the tissues targeted for inflammation in FMF express *MEFV*. In the present study, we investigated resident cells from joint tissues and demonstrated that *MEFV* transcripts and pyrin protein are expressed in synovial fibroblasts (and in dendritic cells), but not in chondrocytes and endothelial cells. The potential of contaminating inflammatory cells being the source of *MEFV* transcripts in synovial fibroblast cultures was minimized by using synovial fibroblasts from passages 4–10. Moreover, we confirmed that all cells in the culture exhibited typical fibroblastic morphology and pyrin staining.

Although the level of *MEFV* transcripts in synovial fibroblasts was lower compared with that seen in unfractionated PBLs, *MEFV* message was consistently up-regulated by treatment with LPS, as has been shown in PBLs (13,14,20). Synovial fibroblasts are biologically

active cells with potential for cytokine and chemokine production; this may allow them to actively participate in the inflammatory process in FMF. Conversely, pyrin expression by synovial fibroblasts may also modulate other inflammatory conditions. Indeed, in a Turkish cohort of patients with juvenile idiopathic arthritis, it was found that the carrier frequency of the M694V allele was significantly higher than in the general population (28). This strong association suggests that pyrin function may affect the expression of chronic idiopathic arthropathies.

Herein we describe 2 previously unrecognized alternative splicing events, involving exon 4a and exon 8ext, that produce frameshifts and predict truncated protein products lacking exons 5–10 and exons 9 and 10, respectively. The exon 8ext transcript is of particular interest since it accounts for up to 27% of the synovial fibroblast transcripts. This transcript encodes a protein similar in structure to native mouse and rat pyrin, which also lack exon 10 (29). This exon encodes the rfp/B30.2/ SPRY domain that is predicted to function in ligand binding or signal transduction (30). The localization of the majority of human FMF mutations to this exon suggests that it encodes a critical part of the molecule. Thus, it is curious that all mouse and rat forms, as well as some human forms of pyrin, lack the domain encoded by this exon. One possibility is that this domain imparts a regulatory function that modulates some basal property of the rest of the pyrin molecule. In this context, it is notable that one FMF mutation (Y668X) encodes a frameshift that results in the loss of half of the rfp domain (31). It is not yet clear whether this partial deletion completely abrogates the function of the rfp domain, but if so, this "natural" model would predict that the basal activity of the rest of the pyrin molecule (and perhaps by extension, that of the exon 8ext protein product) is proinflammatory.

The protein product of the exon 4a transcript resembles the truncated form of pyrin engineered in the context of a mouse model of FMF containing exons 1, 2, and part of exon 3; these mice exhibit a proinflammatory phenotype, with increased IL-1β production and impaired apoptosis (32). Although the exon 4a product is present at very low concentrations, it will be important to learn whether its function resembles that of the truncated mouse form. If so, this product could potentially modulate pro–caspase 1 activation and IL-1β production, as well as apoptosis (32).

Synovial cells also express two *MEFV* splice forms that involve exon 2: one lacking exon 2 (2Δ) and

one in which a small exon is substituted for the canonical exon 2 (2a). Interestingly, comparison of *MEFV* exon 2 in humans and rodents indicates that this is a particularly poorly conserved region of the pyrin protein (29); thus, this region of the pyrin protein may not be under major functional constraints. The exon 2Δ splice form was identified in previous studies and shown to encode a protein product that localizes to the nucleus (27). In our transfection studies, this transcript was the only isoform to encode a nuclear form of pyrin protein. Importantly, proteins encoded by exon 2Δ were not exclusively nuclear and were more often cytoplasmic, suggesting that they may shuttle between these two environments. However, the exon 2Δ (and exon 2a) transcripts were expressed at such low levels in LPS-stimulated synovial fibroblasts and PBLs that their functional significance is unclear. It seems highly unlikely that the rare exon 2Δ nuclear form could account for the native nuclear pyrin protein observed in several cell types, although an unusually stable mRNA or protein could potentially play some role.

The expression of these pyrin protein isoforms also has the potential to affect interactions between pyrin and other proteins. Thus far, pyrin has been shown to interact with 2 proteins, ASC (33) and PSTPIP1/ CD2BP1 (19). ASC is involved in NF-κB activation, caspase 1 activation, and apoptosis, and there are data suggesting that pyrin can modulate each of these functions (32–35). The interaction between pyrin and ASC is mediated by exon 1, the region that encodes the death domain–related pyrin domain of both proteins. Since all splice isoforms identified retain exon 1, all encoded protein forms should retain the ability to interact with ASC, although it is possible that the outcome of this interaction may be different, especially when the truncated forms (4a and exon 8ext) are involved.

The PSTPIP1–pyrin interaction involves the region of pyrin encoded by exons 3–8 (B box and coiled-coil), and could therefore be compromised in the case of the exon 4a form, or altered in affinity or function in the case of the exon 8ext form. Recently, it was demonstrated that PSTPIP1 is mutated in PAPA syndrome (9) and that the 2 major PSTPIP1 mutations functionally affect IL-1β processing and also increase the interaction between pyrin and PSTPIP1 (19). This suggests that these 2 proteins lie in the same inflammatory pathway. Further analysis of possible differences in interaction or functional modulation of these pathways imparted by the different protein isoforms of pyrin is an important future goal since preferential expression of some potentially proinflammatory isoforms may result in the FMF

phenotype in patients with no identified *MEFV* mutations, or may contribute to the inflammatory state in other conditions.

Finally, we have established in this study that native pyrin protein is localized in different subcellular compartments in different cell types. Nuclear localization in synovial fibroblasts, DCs, and PMNs was unexpected since the majority of *MEFV* transcripts found in all of these cell types are full length, and studies of recombinant pyrin in transfected cells, including those described here, have consistently indicated that full-length pyrin is cytoplasmic (27,32,33,36,37). Nuclear localization in synovial fibroblasts was not due to LPS exposure since unstimulated cells also displayed nuclear pyrin. It is likely that mechanisms besides alternative splicing, such as cell-specific posttranslational processing and/or protein–protein interactions, may ultimately determine subcellular localization. The existence of various pyrin isoforms with potentially pro- and antiinflammatory functions, and the observation that native pyrin has a different subcellular localization depending on cell type, indicate that the role of pyrin in the inflammatory process is highly complex and context-specific.

ACKNOWLEDGMENTS

REFERENCES

1. Hull KM, Shoham N, Chae JJ, Aksentijevich I, Kastner DL. The expanding spectrum of systemic autoinflammatory disorders and their rheumatic manifestations. Curr Opin Rheumatol 2003;15: 61–9.

2. Drenth JP, van der Meer JW. Hereditary periodic fever. N Engl J Med 2001;345:1748–57.

3. McDermott MF, Aksentijevich I, Galon J, McDermott EM, Ogunkolade BW, Centola M, et al. Germline mutations in the extracellular domains of the 55 kDa TNF receptor, TNFR1, define a family of dominantly inherited autoinflammatory syndromes. Cell 1999;97:133–44.

4. Hoffman HM, Mueller JL, Broide DH, Wanderer AA, Kolodner RD. Mutation of a new gene encoding a putative pyrin-like protein causes familial cold autoinflammatory syndrome and Muckle-Wells syndrome. Nat Genet 2001;29:301–5.

5. Dode C, Le Du N, Cuisset L, Letourneur F, Berthelot JM, Vaudour G, et al. New mutations of CIAS1 that are responsible for Muckle-Wells syndrome and familial cold urticaria: a novel mutation underlies both syndromes. Am J Hum Genet 2002;70: 1498–506.

6. Aksentijevich I, Nowak M, Mallah M, Chae JJ, Watford WT, Hofmann SR, et al. De novo CIAS1 mutations, cytokine activation, and evidence for genetic heterogeneity in patients with neonatal-onset multisystem inflammatory disease (NOMID): a

7. Drenth JP, Cuisset L, Grateau G, Vasseur C, van de Velde-Visser SD, de Jong JG, et al, International Hyper-IgD Study Group. Mutations in the gene encoding mevalonate kinase cause hyper-IgD and periodic fever syndrome. Nat Genet 1999;22:178–81.

8. Houten SM, Kuis W, Duran M, de Koning TJ, van Royen-Kerkhof A, Romeijn GJ, et al. Mutations in MVK, encoding mevalonate kinase, cause hyperimmunoglobulinaemia D and periodic fever syndrome. Nat Genet 1999;22:175–7.

9. Wise CA, Gillum JD, Seidman CE, Lindor NM, Veile R, Bashiardes S, et al. Mutations in CD2BP1 disrupt binding to PTP PEST and are responsible for PAPA syndrome, an autoinflammatory disorder. Hum Mol Genet 2002;11:961–9.

10. Miceli-Richard C, Lesage S, Rybojad M, Prieur AM, Manouvrier-Hanu S, Hafner R, et al. CARD15 mutations in Blau syndrome. Nat Genet 2001;29:19–20.

11. Samuels J, Aksentijevich I, Torosyan Y, Centola M, Deng Z, Sood R, et al. Familial Mediterranean fever at the millennium: clinical spectrum, ancient mutations, and a survey of 100 American referrals to the National Institutes of Health. Medicine (Baltimore) 1998;77:268–97.

12. Ben-Chetrit E, Levy M. Familial Mediterranean fever. Lancet 1998;351:659–64.

13. The International FMF Consortium. Ancient missense mutations in a new member of the RoRet gene family are likely to cause familial Mediterranean fever. Cell 1997;90:797–807.

14. The French FMF Consortium. A candidate gene for familial Mediterranean fever. Nat Genet 1997;17:25–31.

15. Bertin J, DiStefano PS. The PYRIN domain: a novel motif found in apoptosis and inflammation proteins. Cell Death Differ 2000; 7:1273–4.

16. Martinon F, Hofmann K, Tschopp J. The pyrin domain: a possible member of the death domain-fold family implicated in apoptosis and inflammation. Curr Biol 2001;11:R118–20.

17. Staub E, Dahl E, Rosenthal A. The DAPIN family: a novel domain links apoptotic and interferon response proteins. Trends Biochem Sci 2001;26:83–5.

18. Gumucio DL, Diaz A, Schaner P, Richards N, Babcock C, Schaller M, et al. Fire and ICE: the role of pyrin domain-containing proteins in inflammation and apoptosis. Clin Exp Rheumatol 2002;20 Suppl 26:S45–53.

19. Shoham NG, Centola M, Mansfield E, Hull KM, Wood G, Wise CA, et al. Pyrin binds the PSTPIP1/CD2BP1 protein, defining familial Mediterranean fever and PAPA syndrome as disorders in the same pathway. Proc Natl Acad Sci U S A 2003;100:13501–6.

20. Centola M, Wood G, Frucht DM, Galon J, Aringer M, Farrell C, et al. The gene for familial Mediterranean fever, MEFV, is expressed in early leukocyte development and is regulated in response to inflammatory mediators. Blood 2000;95:3223–31.

21. Matzner Y, Abedat S, Shapiro E, Eisenberg S, Bar-Gil-Shitrit A, Stepensky P, et al. Expression of the familial Mediterranean fever gene and activity of the C5a inhibitor in human primary fibroblast cultures. Blood 2000;96:727–31.

22. Crofford LJ, Tan B, McCarthy CJ, Hla T. Involvement of nuclear factor κB in the regulation of cyclooxygenase-2 expression by interleukin-1 in rheumatoid synoviocytes. Arthritis Rheum 1997; 40:226–36.

23. Reginato AM, Sanz-Rodriguez C, Diaz A, Dharmavaram RM, Jimenez SA. Transcriptional modulation of cartilage-specific collagen gene expression by interferon γ and tumour necrosis factor α in cultured human chondrocytes. Biochem J 1993;294: 761–9.

24. Akman HO, Zhang H, Siddiqui MA, Solomon W, Smith EL, Batuman OA. Response to hypoxia involves transforming growth factor-β2 and Smad proteins in human endothelial cells. Blood 2001;98:3324–31.

25. Morita Y, Yang J, Gupta R, Shimizu K, Shelden EA, Endres J, et al. Dendritic cells genetically engineered to express IL-4 inhibit murine collagen-induced arthritis. J Clin Invest 2001;107:1275–84.

26. Diaz A, Reginato AM, Jimenez SA. Alternative splicing of human prostaglandin G/H synthase mRNA and evidence of differential regulation of the resulting transcripts by transforming growth factor β1, interleukin 1β, and tumor necrosis factor α. J Biol Chem 1992;267:10816–22.

27. Papin S, Duquesnoy P, Cazeneuve C, Pantel J, Coppey-Moisan M, Dargemont C, et al. Alternative splicing at the MEFV locus involved in familial Mediterranean fever regulates translocation of the marenostrin/pyrin protein to the nucleus. Hum Mol Genet 2000;9:3001–9.

28. Ozen S, Bakkaloglu A, Yilmaz E, Duzova A, Balci B, Topaloglu R, et al. Mutations in the gene for familial Mediterranean fever: do they predispose to inflammation? J Rheumatol 2003;30: 2014–8.

29. Chae JJ, Centola M, Aksentijevich I, Dutra A, Tran M, Wood G, et al. Isolation, genomic organization, and expression analysis of the mouse and rat homologs of MEFV, the gene for familial mediterranean fever. Mamm Genome 2000;11:428–35.

30. Henry J, Mather IH, McDermott MF, Pontarotti P. B30.2-like domain proteins: update and new insights into a rapidly expanding family of proteins. Mol Biol Evol 1998;15:1696–705.

31. Notarnicola C, Manna R, Rey JM, Touitou I. Y688X, the first nonsense mutation in familial Mediterranean fever (FMF). Hum Mutat 2001;17:79.

32. Chae JJ, Komarow HD, Cheng J, Wood G, Raben N, Liu PP, et al. Targeted disruption of pyrin, the FMF protein, causes heightened sensitivity to endotoxin and a defect in macrophage apoptosis. Mol Cell 2003;11:591–604.

33. Richards N, Schaner P, Diaz A, Stuckey J, Shelden E, Wadhwa A, et al. Interaction between pyrin and the apoptotic speck protein (ASC) modulates ASC-induced apoptosis. J Biol Chem 2001;276: 39320–9.

34. Dowds TA, Masumoto J, Chen FF, Ogura Y, Inohara N, Nunez G. Regulation of cryopyrin/Pypaf1 signaling by pyrin, the familial Mediterranean fever gene product. Biochem Biophys Res Commun 2003;302:575–80.

35. Masumoto J, Dowds TA, Schaner P, Chen FF, Ogura Y, Li M, et al. ASC is an activating adaptor for NF-κB and caspase-8-dependent apoptosis. Biochem Biophys Res Commun 2003;303: 69–73.

36. Chen X, Bykhovskaya Y, Tidow N, Hamon M, Bercovitz Z, Spirina O, et al. The familial Mediterranean fever protein interacts and colocalizes with a putative Golgi transporter. Proc Soc Exp Biol Med 2000;224:32–40.

37. Mansfield E, Chae JJ, Komarow HD, Brotz TM, Frucht DM, Aksentijevich I, et al. The familial Mediterranean fever protein, pyrin, associates with microtubules and colocalizes with actin filaments. Blood 2001;98:851–9.